Adaptive Emergency Braking for Highway Safety: A Simulation Framework for Performance and Reliability Evaluation

***Abstract*—Highway safety is a critical concern for automated vehicles, particularly in dynamic and high-risk scenarios requiring precise braking and trajectory adjustments. This paper presents a comprehensive evaluation of an Automated Emergency Braking (AEB) system designed to enhance safety in diverse highway conditions. Using a MATLAB Simulink-based test bench, the study explores Car-to-Car Rear Moving, Car-to-Car Rear Stationary, and Car-to-Car Rear Braking scenarios, adhering to ISO 8855 standards and leveraging a 3 Degrees of Freedom (3DOF) vehicle model.**

The analysis highlights the AEB system's ability to mitigate collisions through adaptive Model Predictive Control and dynamic Path Planning, ensuring safe and efficient navigation. Results demonstrate the AEB system's effectiveness in handling challenges such as deadlocks, rapid deceleration, and complex lane-change scenarios while balancing safety and performance trade-offs. Despite its strengths, limitations related to real-world unpredictability and computational demands are acknowledged, with recommendations for future work to refine integration with predictive algorithms and enhance scalability.

This study underscores the importance of advanced AEB systems in improving highway driving safety and provides a robust framework for evaluating their performance in simulated environments. By addressing critical gaps in current research, this work contributes to the development of more reliable and adaptable braking systems for automated highway driving.

***Index Terms*—Automatic Emergency Braking (AEB), Adaptive Model Predictive Control (AMPC), Path Planning and Trajectory Optimization, Highway Safety**

I. Introduction

HIGHWAY driving presents a unique set of challenges for automated vehicles (AVs), where safety and efficiency must be simultaneously prioritized. Among the critical components of Advanced Driver Assistance Systems (ADAS), Automatic Emergency Braking (AEB) systems play a pivotal role in mitigating collision risks by responding to dynamic and complex driving scenarios. The integration of such systems into AVs has demonstrated significant potential in enhancing highway safety, particularly in situations requiring adaptive braking and precise trajectory adjustments [1].

Traditional AEB systems relied on rule-based frameworks, which, although effective in controlled environments, struggled to adapt to real-world complexities such as erratic vehicle behaviors or environmental changes [2]. Modern advancements, leveraging adaptive Model Predictive Control (AMPC) and high-fidelity Path Planning algorithms, have introduced a new dimension of flexibility, enabling AVs to navigate dynamic highway conditions with improved safety and performance. These systems optimize longitudinal and lateral dynamics, ensuring a smooth transition between braking and trajectory corrections.

This study introduces a comprehensive test bench for evaluating AEB systems in diverse highway scenarios. Developed in MATLAB Simulink, the test bench accurately simulates various traffic configurations and evaluates the AEB system's adaptability under realistic conditions. The methodology adheres to ISO 8855 standards for vehicle coordinate systems and employs a 3 Degrees of Freedom (3DOF) model to simulate vehicle dynamics. By exploring scenarios such as Car-to-Car Rear Moving (CCRm), Car-to-Car Rear Stationary (CCRs), and Car-to-Car Rear Braking (CCRb), this work systematically assesses the AEB system's effectiveness across diverse operational conditions. The results underscore the importance of integrating predictive algorithms and adaptive controllers into AEB systems to manage high-risk scenarios. Additionally, they highlight the trade-offs between safety and performance efficiency, offering insights into how advanced braking mechanisms can further enhance the reliability of AVs in real-world applications.

This paper contributes to the development of safer and more adaptable AV systems capable of handling the complex challenges of modern highway environments. It presents several key advancements in the design and evaluation of AEB systems, with a strong emphasis on simulation accuracy, adaptive control strategies, and software quality. The primary contributions can be summarized as follows:

- Development of a Comprehensive Simulation Framework: This work introduces a modular and extensible simulation test bench, developed in MATLAB Simulink, specifically designed for the evaluation of AEB systems in dynamic highway environments. The framework simulates a vehicle model and incorporates realistic highway scenarios, including lane changes, stationary obstacles, and sudden deceleration events. The simulation environment adheres to ISO 8855 standards, ensuring accurate representation of vehicle dynamics and motion.
- Integration of AMPC: An AMPC strategy is implemented to manage both longitudinal and lateral dynamics of the Ego vehicle. This controller enables real-time adjustments to braking intensity and trajectory planning, enhancing the system's capability to avoid collisions in high-risk scenarios, such as traffic deadlocks, abrupt braking by lead vehicles, and dense multi-lane traffic conditions.
- Evaluation of Multi-Stage Braking and Recovery Mechanisms: The proposed system incorporates a hierarchical, multi-stage braking process—Partial Braking 1, Partial Braking 2, and Full Braking—coordinated by the AEB controller to respond to varying levels of risk. Addition-

ally, a Recovery Velocity block facilitates the controlled resumption of the Ego vehicle's target speed following a braking event. This mechanism balances the trade-off between safety and performance efficiency, ensuring smooth reintegration into highway traffic flow after hazard mitigation.

II. Related Work

The AEB systems play a pivotal role in enhancing highway safety [3], by mitigating collisions and adapting to dynamic traffic conditions. This section summarizes key advancements in AEB methodologies, focusing on their evolution, performance metrics, and limitations.

Early AEB systems primarily relied on rule-based frameworks, where braking decisions were predefined using static thresholds, such as Time-to-Collision (TTC). While effective in controlled scenarios, these systems often struggled in real-world conditions due to factors like road friction, tire dynamics, and weather variability [4]. Subsequent research incorporated multi-stage braking systems, as shown in Figure 1, with gradual deceleration to balance safety and passenger comfort, typically characterized by progressive braking phases [5] (e.g., Partial Braking 1, Partial Braking 2, and Full Braking). These models emphasized the trade-offs between minimizing jerk and achieving timely collision avoidance [6], [7].

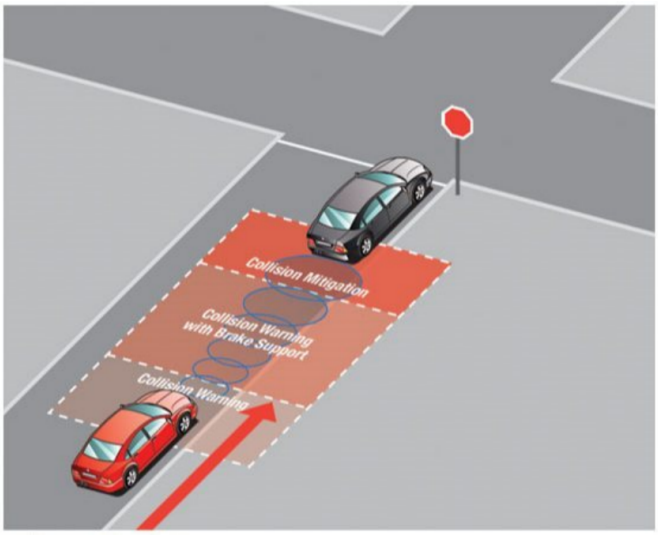

Fig. 1. Illustration of risk evaluation phases in AEB systems. Adapted from [8]

The integration of Path Planning algorithms further enhanced AEB systems by enabling dynamic trajectory adjustments during critical scenarios. High-fidelity models, such as fifth-order polynomial functions, generated smooth, minimum-jerk trajectories, prioritizing collision-free paths [5]. However, these models often faced limitations when confronted with erratic vehicle behavior or sudden environmental changes, highlighting the need for more robust predictive frameworks.

A. Trends and Challenges

Recent advancements in AEB systems [9]–[11] have leveraged machine learning (ML) and artificial intelligence (AI) to address the limitations of traditional models. Deep learning techniques, for instance, have improved the predictive accuracy of collision risks by analyzing historical traffic patterns, while reinforcement learning has dynamically optimized braking strategies in multi-agent environments. Additionally, sensor fusion techniques, combining inputs from LiDAR, radar, and cameras, have enhanced obstacle detection and classification capabilities.

Despite these innovations, significant challenges remain. High computational demands and real-time constraints often limit the deployment of ML-based systems in production vehicles. Furthermore, existing systems struggle to account for the variability and unpredictability of real-world traffic, such as erratic driver behavior or adverse weather conditions. The integration of AEB with other ADAS, like Adaptive Cruise Control (ACC) and Lane Keeping Assist (LKA), remains underexplored, restricting their holistic effectiveness.

Future research should focus on improving the scalability and adaptability of AEB systems, ensuring seamless integration across diverse driving scenarios and vehicle platforms. Addressing these challenges will be essential for advancing the reliability and efficiency of AEB systems in real-world highway environments.

This study addresses an adjusting deceleration values dynamically based on specific driving scenarios, rather than using fixed values for each phase. This adaptive strategy aims to better handle variations in driving conditions while maintaining safety and passenger comfort.

The development and evaluation of an AEB system tailored for highway trajectory planning with adaptive MPC form the core of this research. Sections AEB Algorithm Construction and Simulation, Highway Lane Change Test Bench Development, Path Planning, and Scenarios delineate the comprehensive methodology adopted, integrating theoretical formulation, simulation models, and practical assessments to validate the AEB system's efficacy in multiple highway scenarios.

III. AEB Algorithm Construction and Simulation

The foundational step involves the algorithmic construction of the AEB system, which is crucial for enabling the system to identify potential collisions and execute timely braking maneuvers to mitigate or avoid impacts. This process necessitates a thorough exploration of vehicle dynamics, sensor integration, and decision-making algorithms to ensure precision and reliability. MATLAB Simulink serves as the primary tool for simulating vehicle dynamics, offering a controlled environment to model vehicular motion accurately. This setup allows for iterative testing and refinement of the AEB algorithm, providing insights into its operational effectiveness and areas for enhancement.

The test cases in this approach are based on a combinatorial sampling of vehicle attributes, such as velocity, starting position, and road lane. This setup allows for simulating lane changes and deceleration to mimic scenarios like braking or collisions with target vehicles. All constructed scenarios adhere to the standard AEB ontology defined by EuroNCAP guidelines [12].

In all tested cases, collisions were deemed avoidable provided that the Ego vehicle executed the appropriate actions in time to prevent impact. Scenarios in which a collision is inevitable—regardless of the control strategy—are automatically excluded from this study. These *unavoidable scenarios* are defined as situations where the available time or space is insufficient for any evasive or braking maneuver to prevent a crash. While such conditions are a harsh reality in real-world traffic, they fall outside the scope of this work, which focuses on evaluating the effectiveness of AEB interventions when a response is still viable. Nevertheless, even in borderline situations—where obstacle detection occurs after breaching the minimum safe braking distance—the system enforces a *maximum damage mitigation*.

On the one hand, we followed the SAE J670 standard defining an Earth-fixed coordinate system in which axes are fixed in an inertial reference frame where the angular velocity and linear and angular acceleration are zero. The vehicle coordinate systems are located on the Ego vehicle and placed on the ground, below the rear axle middle. In addition, the Path Planning and simulations adhere to the ISO 8855 standard, which defines the world coordinate system with axes aligned to the traditional and widely used coordinate system. The world coordinate system is also used in the Frenet frames [13] to describe better the movement of a particular solid object moving in a tridimensional space.

On the other hand, the Vehicle Body 3DOF block[1] from the Vehicle Dynamics Blockset of Matlab[2] was used (as standard components without modification) to design and model the Ego vehicle. Typically, road vehicles use the 3DOF model, which characterizes movement freedom through three key vectors: 1) Horizontal displacement, where it can move forward or back, 2) Lateral displacement, where it can move right or left, and 3) Yaw rotation, which describes the object's rotation around the z-axis. The 3DOF model describes an object's motion on a planar surface, encompassing key driving variables such as distance, velocity, acceleration, braking, and steering. Simplifications allow representation as a two-wheeled, single-track, or bicycle model.

In this work, several assumptions are adopted: target vehicles, referred to as Most Important Objects (MIOs), typically travel at a constant forward velocity on a fixed reference path defined by waypoints. While MIOs have initial and final waypoints, additional points are added to simulate lane changes or braking maneuvers in specific test categories. Additional details on vehicle motion and coordinates are detailed in Appendix A.

The stucture of the Vehicle Body 3DOF block is divided into three main components:

1) Lower Level Controller: This block receives the desired acceleration value and converts it into the corresponding throttle force required to achieve it. It also incorporates a tracking lag to simulate the imperfect response of a real vehicle, reflecting the delay typically observed between commanded and actual acceleration.
2) Vehicle Body 3DOF block: Simulink block that serves as the core component for modeling the dynamic behavior of the Ego vehicle in the simulation framework. This block implements a simplified yet realistic vehicle dynamics model that captures the essential longitudinal, lateral, and yaw motions of the vehicle while operating on a planar road surface. The block models the Ego vehicle's dynamic behavior by processing control inputs from the Path Following Controller (PFC), including steering angle, throttle, and braking commands. These inputs determine the vehicle's longitudinal and lateral velocities, as well as its yaw angle, using fundamental vehicle dynamics equations that consider factors such as mass distribution, tire-road friction, and aerodynamic drag. The block outputs key state variables—position, velocity, acceleration, yaw rate, and heading angle—that are essential for the operation of the AEB system, AMPC, and Path Planning modules.
3) Coordinate Change: This coordination is essential for maintaining consistency across the different components of the simulation framework, particularly between the Vehicle Body 3DOF block, the Controller, and the Path Planning modules. The Vehicle Body 3DOF block operates using a coordinate system defined by the SAE J670 standard, where the X-axis points forward, the Y-axis points to the left of the vehicle, and the Z-axis points upward.

All the outputs of this block will represent the vehicle's reaction to a set group of conditions (acceleration and steering angle). After applying those values over one unit of time, the block outputs the vehicle's parameters (position, yam, velocity, etc.).

IV. Highway Lane Change Test Bench Development

A key aspect of the methodology is the development of a test bench for evaluating the AEB system in highway lane-change scenarios. Simulating various highway conditions, including lane configurations and traffic densities, this test environment assesses the system's adaptability and reliability in managing dynamic driving situations.

Thus, the test bench developed in Matlab Simulink must accurately represent a vehicle capable of navigating a highway safely, avoiding collisions, and remaining on the road. As shown in Figure 2, this system is constituted of six major subsystems:

1) Scenario and Environment: Reads map data from the base workspace and outputs map information about lanes, actors, and path references.
2) Path Planning: Complex system that determines the best references of a path that the vehicle should act on by resolving optimization problems according to three ADAS.
3) PFC with AEB: Compute optimal control actions while satisfying all requisites stabilized by the Path Planning subsystem and applying the deceleration force (braking) when safety rules are breached.

[1]https://www.mathworks.com/help/vdynblks/ref/vehiclebody3dof.html
[2]https://www.mathworks.com/products/vehicle-dynamics.html

4) Vehicle Dynamics: Represents the behavior of a rigid object (car) when provided with some stimulus (acceleration and steering).
5) Metrics Assessment: Provide information for a driver dashboard and analyze the collision risk calculations for the AEB system.
6) Visualization: Function that creates a Matlab plot using the inputs from the scenario, environment, and planner systems

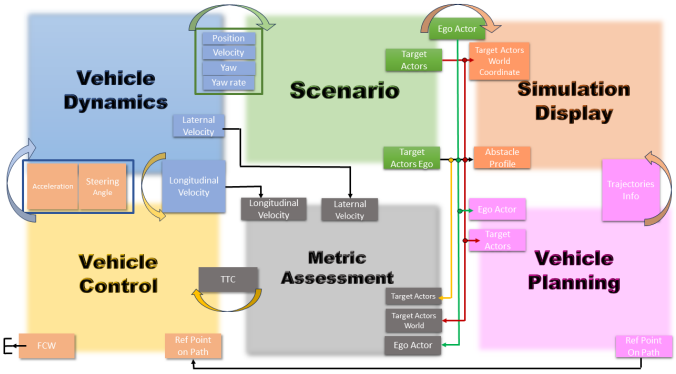

Fig. 2. Highway Lane Change with AEB test bench

The Scenario and Environment block is divided into four components. The Ego vehicle block aims to create a variable representing the primary vehicle which requires data from the Vehicle Dynamic block to define the vehicle's current state. The collision detection system terminates the simulation if the Ego vehicle either leaves the road map or collides with other actors in the environment (such as vehicles or barriers). A collision is detected when the three-dimensional space occupied by the Ego vehicle intersects with that of another object in the scenario, triggering an immediate stop of the simulation.

Furthermore, the two most essential components are the Scenario Reader block (using ISO 8855), which reads a driving scenario from the workspace, providing ground truth about Actors and lane boundaries in Ego vehicle coordinates. Finally, the last block is the Vehicle to World block, which converts target vehicle positions from vehicle to world coordinates. These coordinates will permit the path planning phase to detect the position of other vehicles in the scenario. This block will create the Ego vehicle as a variable and define the positions of the target actor in world coordinates, where these two variables will feed directly to the Path Panning Block.

V. Path Planning

Trajectory planning uses planners to generate a smooth, collision-free trajectory that is recalculated every second of the scenario, considering the environment and road objects.

All vehicle trajectory information is represented by waypoints conjunct, with a minimum of two, first at the starting point (vehicle CG) and final at the road end (simulation ends if CG reaches that point). In these cases, with only two waypoints, the car will travel forward in a straight line with a constant velocity. However, additional waypoints are added to the MIOs to represent lane changes dynamically throughout the scenario. To create a smoother curvature, every lane change is constituted with at least eight waypoints, with yam rotation below eleven degrees.

In any planning process, the ability to project all scenario characters in the world is vital to projecting any solution. For that is used a Frenet coordinate system is a way to represent the position on a road more intuitively than the traditional cartesian coordinates (mathematically more straightforward representation). A six-element row vector represents the global states of a vehicle on cartesian coordinates:

$$globalState = [X, Y, \theta, K, V, A] \tag{1}$$

Where (X, Y) are vehicle position in meters, θ is the orientation angle in radians, K is the curvature in m^{-1}, V is the vehicle velocity in m/s, and A is the vehicle acceleration in m/s^2.

Frenet coordinates use instead variables s and l to describe the vehicle's position, where s represents longitudinal displacement and l represents the lateral displacement. This system aims to describe the kinematic properties of an object moving along a continuous and differentiable curve in a three-dimensional Euclidean space. More specifically, it is defined by the derivatives of the tangent, normal, and binormal vectors of the displacement of the moving object. In this scenario, we present displacement over a plan, so the binomial vector is disregarded. Thus, the Frenet states are a six-element row vector represented by position, velocity, and acceleration relative to a reference path:

$$frenetState = [s, \frac{ds}{dl}, \frac{d^2s}{dl^2}, l, \frac{dl}{ds}, \frac{d^2l}{ds^2}] \tag{2}$$

The high-level motion planning for lane change maneuvers is structured into three core functions: the Dynamic Capsule List, the Reference Path in Frenet coordinates, and the Trajectory Generator in Frenet space [3]. Dynamic Capsule List uses the Simulink functionality, which generates dangerous areas or ovals in turn of a target object. These capsules are created every instant over a determined predicted future trajectory and represent a hazardous zone of a potential collision in each instant of time. Vehicle terminal states with paths that collide or intercept the capsule area are considered to have a low value as an optimal solution. Conversely, Reference Path Frenet [4] converts the coordinates from global coordinates to Fernet coordinates or from Fernet coordinates to global coordinates. Finally, when given a conjunct of terminal states, the Fernet Trajectory Generator produces multiple candidate trajectories that the Ego vehicle can apply to achieve the terminal state that it pretends to reach. All conducted trajectory generation and motion predictions happen in Fernet Space.

The Path Planning system works with Fernet's Coordinates, so Ego vehicle and surrounding MIOs coordinates need to be converted. Then, the Terminal State Sampler will define terminal states according to three major ADAS: Lead Car

[3]https://www.mathworks.com/help/nav/ref/trajectorygeneratorfrenet.html
[4]https://www.mathworks.com/help/nav/ref/referencepathfrenet.html

Following (LCF), Cruise Control (CC), and Lane Change (LC). Being necessary to have potion awareness of Ego vehicles and all safe and non-safe MIOs (based on TTC), to apply all projections according to all the three ADAS. When the current Ego vehicle lane is safe with no MIOs, it will generate a terminal state according to CC. When the current Ego vehicle lane is safe but exists a lead safe-target is used LCF. Finally, in case of an unsafe MIO in the Ego vehicle lane and one of the adjacent lanes is safe, the Terminal Generator Sampler will create terminal states according to the LC. These terminal fernet states will vary according to all possible degree ranges applicable to trajectory curvature. All this process occurs inside the Terminal State Sampler, which occurs inside the Fernet Space.

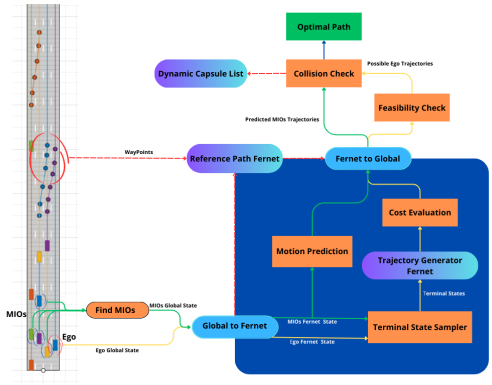

Fig. 3. Schematic of Motion Planner

All terminal states are then sent to the Fernet Trajectory Generator, creating multiple trajectories to achieve these terminal states. These trajectories are sent to a Cost Function and Feasibility Function. Simultaneously, uses predicted target trajectories of MIOs that will be intertwined with Ego vehicle possible trajectories to check for collisions. Ultimately, we will obtain all possible collision-free Ego vehicle trajectories sorted by cost and feasibility. The first element in the list is the optimal trajectory to that specific situation where Ego vehicle finds itself.

In more in-depth analyses, the CC mode has an exclusive focus on longitudinal displacement. This means that the longitudinal position has no restriction (Nan), the Ego vehicle longitudinal velocity will be set Ego vehicle velocity ($\dot{s}_{des}$), and acceleration will be zero. By remaining in the same lane, the terminal state lateral deviation ($l_{expLane}$) will be the lateral offset of the vehicle regarding the Ego vehicle lane center, while lateral velocity and lateral acceleration will be zero. Finally, the number of steps (n-seconds) in the future to predict the terminal state time horizon (t_{hor}).

$$cruiseControlState = [Nan, \dot{s}_{des}, 0, l_{expLane}, 0, 0, t_{hor}] \tag{3}$$

The LCF mode is similar to the previous one. However, there is a safe target in front of the Ego vehicle, so velocity must be regulated to avoid collision with the front target. This means that we need to predict the displacement of the lead vehicle in the time horizon:

$$closetLeadVehicleState = [s_{Lead}, \dot{s}_{Lead}, 0, l_{Lead}, \dot{l}_{Lead}, 0] \tag{4}$$

The terminal state of this mode is calculated based on the notion that the Ego vehicle will mimic the lead vehicle. Still, longitudinal distance needs to subtract a safety distance factor so the terminal state doesn't end up close or inside the danger capsule of the lead vehicle.

$$followLeadVehicleState = (s_{Lead} - s_{safety}), \dot{s}_{Lead}, 0, l_{Lead}, \dot{l}_{Lead}, 0, t_{hor} \tag{5}$$

LC mode corresponds to the terminal states that need to be generated for other adjacent lanes. Any object in front of the Ego vehicle that breaches the distance or velocity safety gap is automatically considered unsafe. The process starts similarly to the previous modes by determining the current Ego vehicle lane, but now, all adjacent left or right (if exit) must also be evaluated. Suppose these lanes are valid or unrestricted of targets. In that case, a similar function of CC is applied, but in that respective lane, when the only difference is that the longitudinal velocity will be equal to the correct velocity instead of the Ego vehicle velocity set for the scenario.

$$cruiseControlState = [Nan, \dot{s}_{cur}, 0, l_{expLane}, 0, 0, t_{hor}] \tag{6}$$

The Motion Planner evaluates all concatenated terminal states and attributes a cost value to each of them, then sorts the states by cost and feeds into a function that produces trajectories for the Ego vehicle. This function will generate multiple candidate Ego vehicle trajectories to reach the terminal states. With the trajectories defined, they filtered through kinematic feasibility functions, where trajectories with an excessive curvature or a yam rate that was too high or too low will be automatically removed. Then feasible trajectories are filtered by removing all collisions. The cost aims to choose the terminal state close to the lane center with a low-velocity variation and the slowest trajectory possible.

$$C_{TOTAL} = C_{latDev} + C_{time} + C_{speed} \tag{7}$$

Penalizing terminal states that deviate too much from the lane center. This is possible using the minimum argument of the lateral deviation between the current Ego vehicle lateral deviation $L_{egoLane}$ and the lateral deviation of any terminal states $L_{terminalState}$. Prioritizing modes that make the Ego vehicle stay in the current Lane.

$$C_{latDev} = W_{\triangle L} * \triangle L \tag{8}$$

$$\triangle L = argmin(|L_{egoLane} - L_{terminalState}|) \tag{9}$$

Relative to time, it prioritizes all the terminal states with a longer time to reach that terminal state. This means that a slower-to-achieve terminal state typically has a smoother curvature.

$$C_{time} = -W_{\triangle t} * \triangle t \tag{10}$$

Finally, the velocity costs prioritize all terminal states that aim to preserve the current Ego vehicle velocity. This is received by the differential of terminal state velocity $v_{terminalState}$ and the Ego vehicle velocity v_{ego}.

$$C_{velocity} = -W_{\triangle v} * \triangle v \tag{11}$$

$$\triangle v = v_{terminalState} - v_{ego} \tag{12}$$

The terminal states are sorted in ascending order, where equations of fifth-order polynomials 13 and 14 are used to generate trajectories with smooth and continuous curvature to retrieve the Ego vehicle motion waypoint.

A possible trajectory can be generated by deriving the equations for longitudinal displacement $s(t)$ and lateral displacement $l(t)$.

$$l(t) = a_6t^5 + a_5t^4 + a_4t^3 + a_3t^2 + a_2t + a_1 \tag{13}$$

$$s(t) = b_6t^5 + b_5t^4 + b_4t^3 + b_3t^2 + b_2t + b_1 \tag{14}$$

Deriving distance, is obtain equations for velocity $\dot{s}(t)$, acceleration $\ddot{s}(t)$, and jerk $\dddot{s}(t)$.

$$\dot{s}(t) = 5a_6t^4 + 4a_5t^3 + 3a_4t^2 + 2a_3t + a_2 \tag{15}$$

$$\ddot{s}(t) = 20a_6t^3 + 12a_5t^2 + 6a_4t + 2a_3 \tag{16}$$

$$\dddot{s}(t) = 60a_6t^2 + 24a_5t + 6a_4 \tag{17}$$

Furthermore, the start boundary conditions at $(t = 0)$ are $s_{start} = a_1, \dot{s}_{start} = a_2, \ddot{s}_{start} = 2a_3$ and $\dddot{s}_{start} = 6a_4$. Therefore, the longitudinal and lateral movement formulations for jerk-optimal trajectory generation are defined as follows:

$$s(t) = \frac{1}{6}\dddot{s}_{start}t^3 + \frac{1}{2}\ddot{s}_{start}t^2 + \dot{s}_{start}t + s_{start} \tag{18}$$

The same is applied to velocity, acceleration, and jerk:

$$\dot{s}(t) = \frac{1}{2}\dddot{s}_{start}t^2 + \ddot{s}_{start}t + \dot{s}_{start} \tag{19}$$

$$\ddot{s}(t) = \dddot{s}_{start}t + \ddot{s}_{start} \tag{20}$$

$$\dddot{s}(t) = \dddot{s}_{start} \tag{21}$$

A trajectory with the best values for velocity, acceleration, and jerk according to these equations, collision-free and feasible, will be defined as the optimal trajectory to be adopted. The collision-free detection is an operation with the highest computational cost because it requires the prediction of MIOs' trajectories in the future. The simulation uses the Dynamic Capsule List object[5], which manages two separate lists of capsule-based collision objects: one representing the Ego vehicle and the other representing surrounding targets.

Automobile (Sedan)	Measures
Length	4.7m
Width	1.8m
Height	1.4m
Wheelbase	2.8m
Front Overhang	0.9m
Rear Overhang	1.0m

TABLE I
SEDAN DIMENSIONS IN SCENARIO DESIGNER

Using the vehicle dimensions provided in Table I, the system generates capsule-based collision objects for the target vehicles. These are used to check for potential collisions between the Ego vehicle and surrounding targets during and between replan cycles. The first valid, collision-free trajectory identified is selected as the optimal trajectory.

A. Path Planning with AEB Controller

The AMPC aims to compute optimal control actions while satisfying all requisites established by the Path Planning subsystem. This will allow us to fulfill the primary goal of automated steering of a car whose lateral vehicle dynamics change with time due to the varying longitudinal velocity. The AMPC predicts future behavior using dynamic models based on linear-time-invariant (LTI) to accumulate the high rate of variables changing over time [14]. This subsystem is divided into two parallel components: the Path Planning Controller and the AEB system.

1) Path Planning Controller: The primary Controller is an upper-level, path-following controller block that aims to keep the vehicle in a marked trajectory while maintaining a user-set velocity. The PFC [6] from Model Predictive Control Toolbox [7] combines the lateral and length longitudinal control using the AMPC. This Simulink out-of-the-box block will generate the longitudinal acceleration and steering angle inputted to the vehicle to perform the desired trajectory. Reduces tuning efforts, supports multivariable (predominant case in this project), better handles constraints, and has a preview capability. It is more efficient in handling the varying dynamics over time, using a constant internal planned model. The PFC also contains a LKA [8], which commands lateral deviation and relative yam angle close to zero, traveling along an imaginary line that represents the center of the lane by adjusting the front steering angle.

In contrast, the longitudinal control module monitors the velocity of the Ego vehicle relative to that of the lead vehicle (if present), adjusting longitudinal acceleration to maintain a safe following distance. This behavior is commonly referred to as ACC [9].

To perform a lane change, the two parts must work simultaneously: lateral and longitudinal controls. The AMPC's ability to accommodate operating conditions over time will allow a

[5]https://www.mathworks.com/help/nav/ref/dynamiccapsulelist.html

[6]https://www.mathworks.com/help/mpc/ref/pathfollowingcontrolsystem.html
[7]https://www.mathworks.com/products/model-predictive-control.html
[8]https://www.mathworks.com/help/mpc/ref/lanekeepingassistsystem.html
[9]https://www.mathworks.com/help/mpc/ref/adaptivecruisecontrolsystem.html

reduced error in accuracy with a fixed plant model structure that changes over a finite prediction horizon. The default Ego vehicle MPC[10] uses plant, disturbance, and noise models for prediction and state estimation, being defined as follows:

$$x(k+1) = Ax(k) + B_u u(k) + B_v v(k) + B_d d(k) \quad (22)$$

$$y(k) = Cx(k) + D_v v(k) + D_d d(k) \quad (23)$$

Where x is a state, k is the time index, u is the manipulated outputs, v is the measured disturbance input, d is the unmeasured disturbance inputs, and y is the output of the system. A is the state matrix, B_u, B_v, B_d, are the input to state matrices of u, v d respectively. C is the state to output matrix, D_v, and D_d are the feedthrough matrices of v and d respectively.

In other words, u corresponds to the vehicle's front wheel steering angle and acceleration (the output controlled by the MPC), while v indicates the previewed curvature. The AMPC also requires an extra input, which contains an updated plant model of the system and the nominal operating point, at which its model applies to obtain the LTI approximation. The updated plant model combines two state-space models: one for ACC and one for LKA. The ACC system controls the velocity of the Ego vehicle using the throttle, which is defined as follows:

$$\ddot{x} = \frac{1}{\tau s + 1} \ddot{x}_{des} \quad (24)$$

Where $\ddot{x}$ is the throttle, $\ddot{x}_{des}$ is the desired acceleration, and τ is the desired acceleration time constant ($\tau = 0.5s$ for analysis and simulation).

This translation of the desired acceleration to throttle is done between the AMPC and the vehicle dynamics, where the throttle will be fed directly to the 3DOF block. Following this, the predictive state-space model for ACC is defined as follows:

$$A_1 = \begin{bmatrix} -\frac{1}{\tau} & 0 \\ 1 & 0 \end{bmatrix}, B_1 = \begin{bmatrix} \frac{1}{\tau} \\ 0 \end{bmatrix}, C_1 = \begin{bmatrix} 0 & 1 \end{bmatrix}, D_1 = 0 \quad (25)$$

In addition, the predictive state-space model for LKA is defined as follows:

$$A_2 = \begin{bmatrix} \frac{-2(C_f + C_r)}{mV_x} & \frac{-V_x - 2(C_f l_f - C_r l_r)}{mV_x} \\ \frac{-2(C_f l_f - C_r l_r)}{I_{zz} V_x} & \frac{-2(C_f (l_f)^2 - C_r (l_r)^2)}{I_{zz} V_x} \end{bmatrix}, \quad (26)$$

$$B_2 = \begin{bmatrix} \frac{2C_f}{m} \\ \frac{2C_f l_f}{I_{zz}} \end{bmatrix}, \quad (27)$$

$$C_2 = \begin{bmatrix} 1 & 0 \\ 0 & 1 \end{bmatrix}, \quad (28)$$

$$D_2 = \begin{bmatrix} 0 \\ 0 \end{bmatrix} \quad (29)$$

[10]https://www.mathworks.com/help/mpc/gs/mpc-modeling.html

All these variables are taken from the Vehicle Dynamic Block, where m is the vehicle total mass, I_{zz} is the yaw moment of inertia, l_f is the longitudinal distance from Ego vehicle CG to front tires, l_r is the Longitudinal distance from Ego vehicle CG to rear tires, c_f is the front tires cornering stiffness, c_r is the rear tires cornering stiffness and V_x is the car longitudinal velocity.

As the PFC system combines these two previous systems, its model results in the following predictive state-space model:

$$A = \begin{bmatrix} A_1 & 0 \\ 0 & A_2 \end{bmatrix} \quad (30)$$

$$B = \begin{bmatrix} B_1 & 0 \\ 0 & B_2 \end{bmatrix}, \quad (31)$$

$$C = \begin{bmatrix} C_1 & 0 \\ 0 & C_2 \end{bmatrix}, \quad (32)$$

$$D = \begin{bmatrix} D_1 & 0 \\ 0 & D_2 \end{bmatrix}, \quad (33)$$

2) AEB system: The AEB controller uses TTC calculation to evaluate scenarios and determine when to perform a longitudinal deceleration until the car stops. Using a stopping time calculation approach, the AEB Controller implements the Forward Collision Warning (FCW) and three braking stages:

$$T_{stop} = \frac{V_{ego}}{\alpha_{brake}} \quad (34)$$

Where T_{stop} refers to the time until the vehicle becomes stationary, V_{ego} longitudinal velocity of the Ego vehicle, and α_{brake} is the standard brake acceleration applied in the particular state.

In other words, it calculates the necessary time for a specific deceleration force to stop a vehicle traveling at a determined velocity entirely. This value is later compared to TTC off the vehicle and the forward vehicle to classify the correct braking state where the car finds itself and acts accordingly.

The AEB subsystem employs a three-stage braking strategy—Partial Braking 1 (PB1), Partial Braking 2 (PB2), and Full Braking (FB)—designed to progressively escalate deceleration based on the severity of risk. This approach balances early intervention with passenger comfort and adheres to industry best practices for AEB calibration, including deceleration thresholds observed in real-world emergency braking scenarios. Each stage is associated with a predefined deceleration value: PB1 at 5.8 m/s, PB2 at 7.3 m/s, and FB at 9.8 m/s. Additionally, the FCW system is configured to trigger at a deceleration threshold of 4 m/s.

The previous equation is used to determine the times to stop the car for every stage, plus an error margin and one second (one pulse generator cycle). This inadvertently allows the entire system in the loop to have one more chance to check all parameters and go back through the process, especially giving Path Planner chances to design new alternative paths. The FCW works independently from braking stages and is generally activated before braking. Still, it is also possible to

appear when the vehicle realizes it needs to start the full brake immediately, and the FCW is activated simultaneously, which occurs when target vehicle suddenly cuts to the front of the Ego vehicle (a test case scenario). The calculation of FCW is based on a derivation of the main formula:

$$T_{FCW} = T_{reaction} + \frac{V_{ego}}{\alpha_{brake}} \tag{35}$$

It adds the time that the driver needs to react to the illumination of the warning signal $T_{reaction}$, which is defined as approximately 1.2 seconds. The objective is for the FCW signal to be activated before the PB1 and remain activated to all braking states (PB1, PB2, FB), only being turned off when the car leaves a dangerous situation, or the vehicle successfully executes the braking maneuver to stop and the car finds itself full immobile.

The AEB systems will be divided into two steps: the first calculates the times-to-stop T_{stop}. The second subsystem aims to compare and analyze the state's situation based on TTC and the times-to-stop. After classifying the state and determining the corrective deceleration state that needs to be applied at that time state.

The braking system operates in three consecutive stages, transitioning gradually under normal conditions. However, rapid changes in the environment, such as vehicles cutting in or sudden braking by a lead vehicle, may require skipping stages. In more dangerous scenarios, the system may bypass PB1 or activate the FB stage directly to apply rapid deceleration. The FCW is triggered alongside Partial Brake 1 or bypassed entirely in extreme situations. These adjustments depend on the PFC's ability to execute alternative steering maneuvers to prevent collisions.

On the other hand, the Recovery Velocity block is activated after a partial braking event, once the driving scenario has evolved—typically when the PFC identifies a safer adjacent lane or completes a lane change. If the deceleration during the maneuver was substantial, causing the following vehicle to overtake the Ego vehicle, this block facilitates the recovery of lost momentum. It gradually increases the Ego vehicle's longitudinal velocity, aiming to close the gap between its current speed and the predefined target velocity. Once the velocity approaches the desired threshold, control is handed back to the MPC. However, if the newly selected lane remains unsafe, the acceleration process is suspended, and the MPC continues to maintain full control to ensure safety.

Unlike the vehicle's primary Path Planning system, which continuously predicts and adjusts for potential conflicts, the AEB module does not engage in long-term trajectory prediction. Instead, it operates as a reactive safety mechanism that monitors real-time driving conditions and responds based on predefined thresholds, such as TTC and distance gaps. This design ensures rapid intervention in emergency scenarios, reinforcing the AEB system's role as a last line of defense when proactive avoidance is no longer feasible.

B. Metrics Assessments and Visualization

Metrics assessments provide a quantitative analysis of the system's effectiveness, focusing on key performance indicators such as collision avoidance rate, braking efficiency, and system responsiveness. Visualization, alternatively, offers a qualitative perspective by graphically representing the system's operation during simulated lane-changing events on the highway. This approach facilitates a nuanced understanding of the AEB system's functionality, highlighting its operational strengths and pinpointing potential improvements.

The Metrics Assessment is responsible for calculating TTC (used in the AEB), Time Gap, Longitudinal Jerk, and Lateral Jerk (that are displayed for the driver) from information provided by diverse systems in the test bench. One important block is the Detect Lead Vehicle, which computes the distance between Ego vehicle and lead vehicle, also known as headway. The time gap is calculated using the distance to the lead vehicle $d_{headway}$ and the longitudinal velocity v_s of the Ego vehicle.

$$t_{gap} = \frac{d_{headway}}{v_s} \tag{36}$$

The longitudinal jerk $\ddot{v}_s$ is calculated using the derivation of the longitudinal velocity, and the lateral jerk $\ddot{v}_l$ is computed using the derivation of the lateral velocity. Both metrics are compared to standard safe values, and if those values breach safety standards, the lamp in the dashboard corresponding to them will turn red, signaling that violation.

Longitudinal headway is the distance between the vehicle's rear axles reduced by the distance of the Ego vehicle rear axle to the front Ego_{rF} and reduced by the distance of the MIO rear axle to the rear Mio_{rF}. This phenomenon happens because the origin offset is the relative position [x,y] of the vehicle center concerning the rear axle. In contrast, the distance of the rear axle center to the vehicle center is equal to a negative origin offset $Ego_{offeset}$. The longitudinal headway is the distance from the front of the Ego vehicle to the rear of MIO, while the entire system tracks the vehicle position according to his CG. We must determine the front of the Ego vehicle and the rear of the lead vehicle:

$$Ego_{rF} = \frac{Ego_{len}}{2} + Ego_{offeset} \tag{37}$$

$$Mio_{rF} = \frac{Mio_{len}}{2} - Mio_{offeset} \tag{38}$$

$$headway = d - Ego_{rF} - Mio_{rF} \tag{39}$$

Where Ego_{len} and Mio_{len} are the length of the vehicle according to scenario data, and d is the distance between the vehicle's rear axles.

More importantly, with the headway distance of any vehicle ahead and in the Ego vehicle lane, with information about the lead vehicle longitudinal velocity of the target leading vehicle. With all data reunited about Ego vehicle and lead vehicle, it is possible to calculate TTC using the following equation:

$$TTC = \frac{d_{rel}}{v_{rel}} \tag{40}$$

Where TTC in seconds is the time necessary with the current velocity and distance of both vehicles until a collision occurs, d_{rel}, which corresponds to the relative distance,

including the lateral and longitudinal distance between the Ego vehicle and the lead vehicle, and V_{rel} which corresponds to relative velocity including lateral and longitudinal velocity between the Ego vehicle and MIO.

All vehicles in the simulation drive at a constant velocity, without acceleration or deceleration, and always in forward motion—an approach typically used to model highway driving scenarios. However, there are some exceptions in the test cases scenarios 5 and 6 with accident collisions, where abrupt changes in speed between the colliding cars imply a high negative acceleration value for these vehicles due to their collision. The same is applied in cases of CCRb when some vehicles suddenly applied an abrupt or gradual value of declaration, or even in CCRs cases where some of the cars find themselves stationary.

To calculate the magnitude of the distance and velocity vectors between both vehicles (relative distance and velocity), we take advantage of the function from Matlab called *cart2pol*. This function uses polar coordinates to generate the magnitude vectors and their respective angles. The relative velocity angle is the yaw angle, which is the angle from the center line of a lane about the longitudinal velocity, as shown in Figure 4.

$$v_x = v * \cos(\theta_{yam}) \tag{41}$$

$$\theta_{yam} = \theta_{vel} - \theta_{dist} \tag{42}$$

where v_x is the longitudinal velocity, θ_{yam} is the relative yaw angle, θ_{vel} is the velocity angle, and θ_{dist} is the relative distance angle.

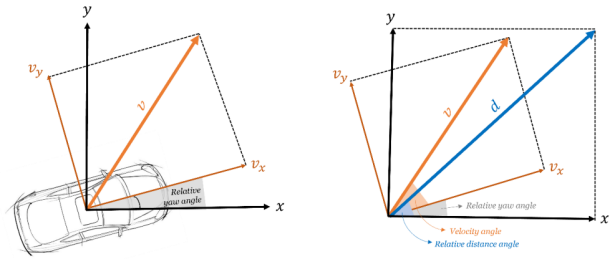

Fig. 4. Relative velocity angle and the relative distance angle

This allows us to extract the relative velocity and distance between the Ego vehicle and the lead vehicle. Then, we can feed it to the function to calculate the TTC (Eq. 40), which will be provided directly to the AEB system inside the Controller block.

VI. Scenarios

This study aims to evaluate the performance of AEB systems in AVs across three distinct yet interrelated highway scenarios. These scenarios are specifically designed to assess the system's ability to manage vehicle maneuvers and respond to dynamic traffic conditions commonly encountered in highway environments, including sudden braking by lead vehicles, stationary obstacles, and complex lane-change maneuvers in dense traffic. These scenarios were carefully chosen to provide a comprehensive evaluation of the AEB system's performance in varying rear-end collision situations, ensuring the assessment of its capability to handle critical safety events representative of real-world highway challenges.

A. Scenario#1

This scenario consists of a four-lane highway. With lane changes, vehicle 1 turns to the right (between 260m and 288m), just like vehicle 4, which only makes the lane change between 340m and 370m. Vehicle 5 makes two lane changes, the first to the right (between 300m and 334m) and again to the right (between 400m and 425m), thus moving into the rightmost lane. Finally, vehicle 9 passes to the right between 520m and 549m. Regarding the CCRs category, vehicle 10 is added at the rightmost lane, where it is stationary 120m from the highway, and to avoid collision with it, vehicle 7 makes two lane changes, one to the left (between 92m and 116m) and the next to the right (between 128m and 160m), returned to the lane from which it started. In the CCRb tests, two cars are braking: vehicle 7 in the rightmost lane (between 210m and 223m) and vehicle 8 in the center-right lane (between 140m and 170m). To avoid collision between vehicles, car 2 has to make two lane changes to avoid an accident, the first to the left (110m and 136m) and then to the left (180m and 204m), returning to the initial lane.

5

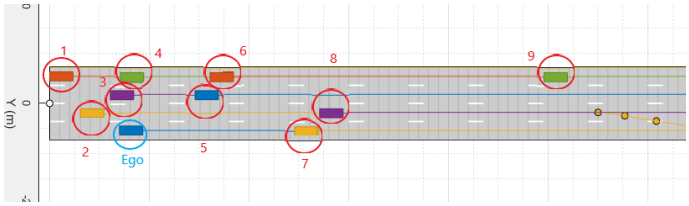

Fig. 5. Lane Change and Braking Dynamics in Scenario#1

B. Scenario#2

This example consists of one variance of Scenario#1 with some changes in the initial positions of some vehicles' positions and longitudinal velocity, plus additional lane changes (this scenario has the highest number of lane changes and waypoints). Vehicle 1 changes lanes to the right (319m and 344m), and vehicle 3 changes lanes to the left (260m and 292m). Vehicle 4 makes two turns, one to the left (between 220m and 256m), followed by one to the right (between 283m and 307m), returning to the rightmost lane. On the other hand, vehicle 5 makes two turns, the first to the right (between 70m and 102m) and the second to the left (between 180m and 206m). Vehicle 6 makes only one turn to the right (between 120m and 153m), and finally, vehicle 8 also turns into the rightmost lane (between 71m and 101m). In the case of CCRs tests, a stationary obstacle (vehicle) is added in the central lane on the right, close to 210m. In addition, lane changes are added to avoid collisions, as is the case with vehicle 2, which has to turn into the rightmost lane between 179m and 204m to avoid collision with the immovable object. Finally, in the

case of CCRb, it is vehicle 8 that makes an emergency braking after changing lanes close to 120m right in front of vehicle ego.

6

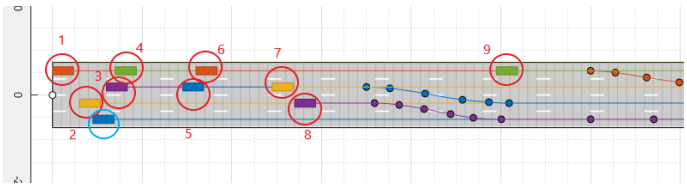

Fig. 6. Lane Change and Braking Dynamics in Scenario#2

C. Scenario#3

This scenario represents an entry ramp between a two-lane highway and a simple one-lane road. The secondary road starts at the coordinates [32.2, -111.8] and intersects the highway near the coordinates [195, 3.6] with the vehicle 2 leading the vehicle 1. However, vehicle 1 adjusts the lateral displacement according to the center line of the rightmost lane to enter the highway, and these curves occur between 193m and 220m. Furthermore, it also presents a higher longitudinal velocity than vehicle 2, so it needs to execute a lane change to the left to avoid collision (between 390m and 420m). For the category CCRs, vehicle 2 is stationary in the rightmost lane, close to 186m (before the entry ramp). In the category CCRb, vehicle 2 starts on position [76, -1.8], executes a slow brake process close to 166m, and ends up close to the entry ramp.

VII. Results and Discussion

The results were aggregated by category and scenario, with each scenario denoted by the letters A to D, representing velocities of 18 m/s, 20 m/s, 22 m/s, and 24 m/s, respectively.

A. Car-to-Car Rear Moving (CCRm)

This category examines scenarios where all vehicles maintain a constant longitudinal velocity, focusing on collisions that occur in systems without AEB. The goal is to compare the performance of AV systems with and without AEB.

While the Ego vehicle's behavior is generally similar in both systems, the AEB-equipped system shows slightly reduced performance. This difference arises because non-AEB systems prioritize speed and optimal highway driving by ignoring proximity risks and assuming consistent trajectories of other vehicles. In contrast, AEB prioritizes safety by intervening when the Ego vehicle approaches a critical distance to a lead vehicle.

AEB applies partial braking to match the lead vehicle's velocity, delaying progress while waiting for safer conditions or lane-change opportunities. Although this safety-first strategy slows the Ego vehicle compared to non-AEB systems, it highlights the trade-off between performance efficiency and realistic, secure driving dynamics.

The CCRm scenarios highlight the critical role of the AEB system in managing varying complexities and ensuring safety through adaptive braking and lane-change strategies. In CCRm1A, no AEB intervention is required as both models behave identically, with no critical situations present. In CCRm1B, the Ego vehicle uses lane changes and partial braking to avoid collisions, with AEB managing proximity to other vehicles. Non-AEB models exhibit unsafe behaviors in such scenarios. In CCRm1C, increased Ego vehicle velocity results in earlier and rapid lane changes. AEB adapts effectively, managing cascading maneuvers to ensure safety despite compressed events. CCRm1D introduces deadlocks, where the AEB system successfully handles these challenges by braking to avoid collisions and enabling safe lane changes, while non-AEB models fail to navigate such situations.

The CCRm2 scenarios showcase the AEB system's ability to handle low to moderate complexity. In CCRm2A and CCRm2B, the Ego vehicle operates at low velocities, with AEB ensuring safe distances through partial braking in CCRm2B. In CCRm2C, slightly stronger braking is required to clear obstructed paths, with AEB ensuring control and smooth transitions. CCRm2D (as depicted in Figure 7) presents a complex deadlock scenario, where AEB manages the situation by braking to create opportunities for safe lane changes and navigating hazardous maneuvers effectively.

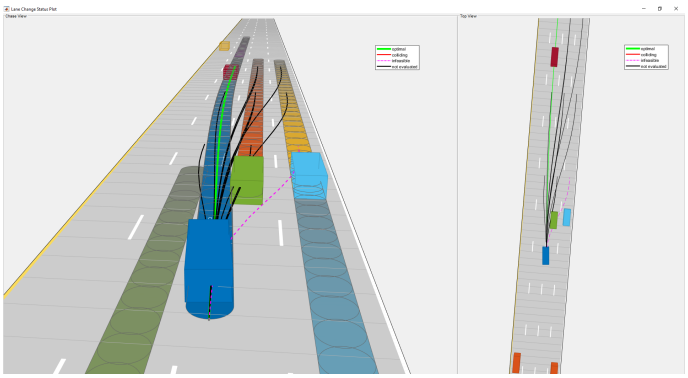

Fig. 7. Data visualization for CCRm2D

In the CCRm3 scenarios, the AEB system demonstrates its ability to handle progressively more challenging situations. In CCRm3A and CCRm3B, no critical interventions are necessary, as the scenarios remain low in complexity. However, in CCRm3C, the AEB system successfully navigates deadlocks through controlled braking and adaptive lane changes, while non-AEB models collide due to insufficient braking capabilities. In CCRm3D, AEB manages lateral and lead vehicle proximity challenges, enabling safe lane changes and maintaining safety, whereas non-AEB models face collision risks due to their inability to adapt.

Overall, as depicted in Table II, the CCRm scenarios emphasize the effectiveness of the AEB system in adapting to dynamic traffic conditions, managing deadlocks, and ensuring safety through timely braking and strategic maneuvers. This highlights the critical importance of AEB in achieving both collision avoidance and reasonable performance across various driving environments.

Scenario	Role of AEB	Limitations Without AEB
CCRm1	- AEB adapts to increasing velocity, dynamic traffic conditions, and potential deadlocks, ensuring safety through strategic maneuvers.	- Non-AEB models fail in complex scenarios, such as CCRm3D, leading to collisions and unsafe behavior.
CCRm2	- AEB ensures safety in varying complexities through timely braking, enabling the Ego vehicle to navigate challenging situations and maintain safe distances.	- Occasional reductions in performance efficiency due to prioritizing safety over speed and trajectory optimization.
CCRm3	- AEB manages progressive challenges, effectively handling deadlocks, avoiding collisions, and maintaining safety through controlled braking and lane changes.	- Non-AEB models cannot adapt to dynamic interactions, leading to collisions in more complex scenarios like CCRm3C and CCRm3D.

TABLE II
SUMMARY OF KEY OBSERVATIONS ON CCRM SCENARIOS

Scenario	Role of AEB	Limitations Without AEB
CCRs1	- AEB mitigates collisions in dynamic environments by avoiding stationary objects and responding to rapid position changes.	- Non-AEB models struggle with adapting to rapid traffic shifts, increasing collision risk.
CCRs2	- AEB prioritizes safe distances, controlled braking, and lane changes in unpredictable scenarios.	- Non-AEB models often execute dangerously close maneuvers, posing significant safety risks.
CCRs3	- AEB ensures adaptive behavior, maintaining safe gaps and enabling lane changes in dynamic conditions.	- Non-AEB models fail to adjust to evolving conditions, relying on minimal gaps and risking collisions.

TABLE III
SUMMARY OF KEY OBSERVATIONS ON CCRS SCENARIOS

B. Car-to-Car Rear Stationary (CCRs)

This category focuses on scenarios with a significantly increased demand for braking, particularly those involving deadlocks. A deadlock arises when the Ego vehicle encounters a stationary object in its lane while adjacent lanes are occupied by non-safe vehicles, preventing the Path Planning system from generating viable alternative trajectories. In such situations, the Ego vehicle is forced to perform a full stop to avoid a collision.

These findings underscore the importance of braking systems in high-risk scenarios and demonstrate the AEB system's critical role in ensuring safety and adaptability under complex traffic conditions.

In the CCRs1 scenarios, the Ego vehicle responds to stationary obstacles and dynamic traffic with braking and lane changes. At higher speeds (CCRs1B), more lane-change attempts occur, though some are canceled due to traffic unpredictability. CCRs1C features two variants: one with successful avoidance and one where only the AEB system prevents a collision. In CCRs1D, stronger initial braking slows the vehicle, enabling recovery and a quicker simulation finish.

In the CCRs2 scenarios, the Ego vehicle responds to stationary vehicles and dense traffic through coordinated braking and lane changes. In CCRs2A, no AEB is required as the vehicle safely cancels and later performs a lane change. CCRs2B and CCRs2C rely on AEB to maintain safe distances, with non-AEB models showing unsafe proximity. CCRs2D involves multiple lane changes and braking actions, demonstrating the system's ability to ensure both safety and efficient navigation.

In the CCRs3 scenarios, the Ego vehicle consistently uses braking and lane changes to avoid stationary vehicles. CCRs3A and CCRs3B show straightforward, safe behavior. CCRs3C highlights the AEB system's ability to maintain safer distances, while non-AEB models operate with unsafe gaps. In CCRs3D, under high-speed and limited maneuverability, AEB enables collision avoidance through timely braking, whereas non-AEB models result in collisions.

As summarized in Table III, these observations highlights AEB's role in adapting to dynamic conditions, ensuring safe braking, and enabling lane changes, particularly in complex scenarios.

C. Car-to-Car Rear Braking (CCRb)

This category examines scenarios where target vehicles perform braking maneuvers, resulting in a significant increase in the number of stops required by the Ego vehicle compared to scenarios with constant longitudinal velocity.

Unlike the previous category, target vehicles here exhibit dynamic velocity changes, following consistent deceleration patterns. This variability challenges the Many Independent Objectives (MIO) system, which typically assumes targets will maintain their current velocity to reduce computational costs. While effective in scenarios with minimal velocity changes, this assumption becomes invalid during rapid braking by lead vehicles.

These dynamics complicate the Ego vehicle's decision-making, requiring increased reactive measures such as braking and trajectory adjustments. The adaptive capabilities of systems like AEB are crucial to handling such scenarios, addressing the challenges posed by rapid deceleration and ensuring safe navigation. Individual test cases provide further insights into these complexities.

In the CCRb1 scenarios, the AEB system enables safe braking and lane changes under sudden deceleration events. In CCRb1A, AEB supports controlled avoidance of vehicle 8, while non-AEB models follow aggressive paths. CCRb1B and CCRb1C involve deadlocks; AEB allows full braking to avoid collisions, but non-AEB models fail. In CCRb1D, AEB facilitates smooth lane changes and cruise control, while non-AEB models show delayed and less effective responses.

In the CCRb2 scenarios, the AEB system consistently enables safe responses to sudden cut-ins and high-speed challenges. In CCRb2A, it prevents rear-end collisions when vehicle 8 merges abruptly. CCRb2B and CCRb2C involve complex lane changes, where AEB ensures safe maneuvering and braking, while non-AEB models struggle with trajectory conflicts. In CCRb2D, despite limited lane-change options at high speed, AEB effectively avoids collisions, whereas non-AEB models fail under deadlock conditions.

In the CCRb3 scenarios, the Ego vehicle manages braking and lane changes with varying complexity. CCRb3A

involves straightforward maneuvers without requiring AEB. In CCRb3B and CCRb3C, increased velocity in CCRb3C heightens deceleration demands, highlighting AEB's role in maintaining safe gaps. In CCRb3D (Figure 8), AEB successfully prevents collisions by synchronizing braking with the lead vehicle, whereas non-AEB models fail due to delayed reactions.

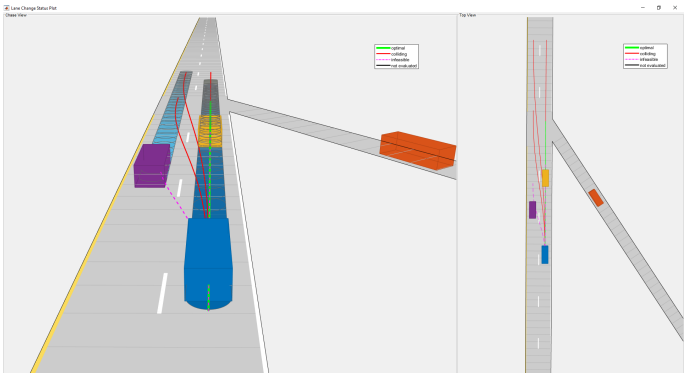

Fig. 8. Data visualization for CCRb3D

These observations, as summarized in Table IV, highlights AEB's effectiveness in managing braking, deadlocks, and lane changes, particularly in scenarios involving complex traffic dynamics, while contrasting the unsafe and collision-prone behavior of non-AEB models.

Scenario	Role of AEB	Limitations Without AEB
CCRb1	- AEB ensures collision avoidance through timely braking, even in deadlock scenarios.	- Non-AEB models exhibit unsafe and collision-prone behavior due to inadequate braking and impasse handling.
CCRb2	- AEB effectively manages complex situations, ensuring safe braking, avoiding collisions, and adapting to dynamic lane changes.	- Non-AEB models fail to respond adequately, leading to collisions, especially in cases like CCRb2A.
CCRb3	- AEB adapts to high velocities and dense traffic, maintaining safe distances and preventing collisions.	- Non-AEB models struggle with limited lane-change opportunities and cannot prevent collisions in critical scenarios.

TABLE IV
SUMMARY OF KEY OBSERVATIONS ON CCRB SCENARIOS

D. Key Observations

Tables V and VI summarize the key findings across the tested scenarios, highlighting the comparative performance and limitations of AV systems with and without AEB in dynamic highway environments.

Scenario Category	Non-AEB Model	AEB Model
CCRs	62.5%	100%
CCRs	71%	100%
CCRb	75%	100%

TABLE V
COLLISION AVOIDANCE RATE (%) ACROSS SCENARIOS FOR AEB AND NON-AEB MODELS

VIII. THREATS TO VALIDATION

The study's reliance on simulation-based environments presents a significant limitation, as it may not fully replicate the complexities and unpredictability of real-world driving conditions. Simplified vehicle dynamics, such as the 3DOF model, omit critical factors like lateral forces, tire dynamics, and road irregularities, potentially limiting the system's applicability in practical scenarios. Additionally, the predefined test cases assume controlled target vehicle behaviors and fixed paths, which may not reflect the variability and unpredictability of human-driven vehicles. Moreover, the validation is also limited to comparisons with non-AEB models, leaving room for further benchmarking against other ADAS.

IX. CONCLUSIONS

This study presented a comprehensive evaluation of an AEB system specifically designed for highway scenarios, emphasizing its critical role in enhancing safety and adaptability in dynamic and high-risk driving conditions. Through extensive simulations of various highway configurations and traffic densities, the results demonstrated the AEB system's effectiveness in mitigating collisions via timely interventions, such as adaptive braking and dynamic trajectory adjustments.

The AEB-equipped model consistently outperformed the non-AEB model across all tested scenarios and velocities. Notably, it achieved a 100% collision avoidance rate in low-velocity CCRm and CCRs scenarios. While performance decreased slightly at higher speeds—primarily due to reduced reaction times and complex vehicle interactions—the AEB system maintained superior safety, significantly lowering collision rates compared to the non-AEB model. The system proved particularly effective in managing scenarios involving stationary vehicles and sudden braking events, where rapid and precise interventions were essential.

The analysis also highlighted the AEB system's ability to handle complex scenarios, including rapid deceleration, deadlocks, and multi-lane changes. While these interventions occasionally introduced trade-offs, such as delayed velocity recovery, they consistently prioritized safety and maintained stable driving dynamics.

However, limitations were identified in scenarios requiring rapid decision-making, where the predictive accuracy of the Path Planning system was challenged by abrupt environmental changes. Enhancing the coordination between braking mechanisms and trajectory planning is necessary to further improve system responsiveness under extreme conditions.

Future work will focus on refining the integration of advanced Path Planning strategies and predictive algorithms to address these challenges. Key areas for improvement include handling unpredictable target vehicle behavior, modeling more complex vehicle dynamics, and accounting for varying environmental factors. These enhancements aim to increase the system's reliability, adaptability, and efficiency in managing the complexities of real-world highway driving.

Scenario Category	Key Characteristics	Ego Vehicle Behavior	Challenges
CCRm	• Lead vehicles travel at relatively low velocities. • No stationary objects in the Ego lane. • Ego maintains a safe distance via small braking maneuvers.	• Applies partial braking to adjust velocity. • Explores alternative lanes as they become available. • Maintains flow without requiring full stop.	• Simpler scenarios due to absence of lane-blocking objects. • Limited need for aggressive braking or replanning.
CCRs	• Stationary vehicles present in the Ego lane. • Adjacent lanes often occupied by moving vehicles. • Increased likelihood of deadlock conditions.	• Predicts paths to avoid stationary obstacles. • Executes braking based on gap thresholds. • May stop completely if no safe lane is available.	• Stationary objects complicate planning and avoidance. • Limited maneuverability increases AEB dependence.
CCRb	• Lead vehicles decelerate abruptly. • High deceleration rates introduce sudden risks. • Velocity changes are non-linear and unpredictable.	• Dynamically adjusts speed via AEB. • May execute full braking depending on gap evolution. • Reacts to velocity breach more than spatial blockage.	• Sudden braking disrupts planner's trajectory forecasts. • Requires close coordination between planner and AEB.
General Challenges	• Constant adaptation to unpredictable target behaviors. • Braking must be harmonized with trajectory generation. • Real-time decision-making under uncertainty.	• Balances safety and performance under constraint. • Reacts effectively while minimizing passenger discomfort.	• Trade-offs between planner reactivity and AEB control. • Difficulty in maintaining smooth long-term navigation.

TABLE VI
SUMMARY OF CCR SCENARIO CATEGORIES AND CORRESPONDING EGO VEHICLE BEHAVIOR AND CHALLENGES

ACKNOWLEDGMENTS

This work was supported by FCT/MCTES through national funds and when applicable co-funded EU funds under the project UIDB/50008/2020.

REFERENCES

[1] A. Morgado, C. Gonçalves, and N. Pombo, "Enhancing autonomous vehicles: An experimental analysis of path planning and decision-making processes through simulink-based architecture," in *2023 IEEE 17th International Conference on Application of Information and Communication Technologies (AICT)*, 2023, pp. 1–9.

[2] Y. Zhang, A. Carballo, H. Yang, and K. Takeda, "Perception and sensing for autonomous vehicles under adverse weather conditions: A survey," *ISPRS Journal of Photogrammetry and Remote Sensing*, vol. 196, p. 146–177, Feb. 2023. [Online]. Available: http://dx.doi.org/10.1016/j.isprsjprs.2022.12.021

[3] Y. Fu, C. Li, F. R. Yu, T. H. Luan, and Y. Zhang, "A decision-making strategy for vehicle autonomous braking in emergency via deep reinforcement learning," *IEEE Transactions on Vehicular Technology*, vol. 69, no. 6, pp. 5876–5888, 2020.

[4] L. Yu, R. Wang, and Z. Lu, "Autonomous emergency braking control based on inevitable collision state for multiple collision scenarios at intersection," in *2021 American Control Conference (ACC)*, 2021, pp. 148–153.

[5] W. Zhou and X. Wang, "Calibrating and comparing autonomous braking systems in motorized-to-non-motorized-vehicle conflict scenarios," *IEEE Transactions on Intelligent Transportation Systems*, vol. 23, no. 11, pp. 20 636–20 651, 2022.

[6] D. Wang, K. Nazem Tahmasebi, and D. Chen, "Integrated control of steering and braking for effective collision avoidance with autonomous emergency braking in automated driving," in *2022 30th Mediterranean Conference on Control and Automation (MED)*, 2022, pp. 945–950.

[7] K. Yoneda, T. Iida, T. H. Kim, R. Yanase, M. Aldibaja, and N. Suganuma, "Trajectory optimization and state selection for urban automated driving," vol. 23, no. 4, 2018, p. 474–480.

[8] D. Katare and M. El-Sharkawy, "Embedded system enabled vehicle collision detection: An ann classifier," in *2019 IEEE 9th Annual Computing and Communication Workshop and Conference (CCWC)*, 2019, pp. 0284–0289.

[9] M. Morsali, E. Frisk, and J. Åslund, "Spatio-temporal planning in multi-vehicle scenarios for autonomous vehicle using support vector machines," *IEEE Transactions on Intelligent Vehicles*, vol. 6, no. 4, pp. 611–621, 2021.

[10] Y. Dong, Y. Zhong, and J. Hong, "Knowledge-biased sampling-based path planning for automated vehicles parking," *IEEE Access*, vol. 8, pp. 156 818–156 827, 2020.

[11] H. Chen and X. Zhang, "Path planning for intelligent vehicle collision avoidance of dynamic pedestrian using att-lstm, msfm, and mpc at unsignalized crosswalk," *IEEE Transactions on Industrial Electronics*, vol. 69, no. 4, pp. 4285–4295, 2022.

[12] F. Klück, F. Wotawa, G. Neubauer, J. Tao, and M. Nica, "Analysing experimental results obtained when applying search-based testing to verify automated driving functions," in *2021 8th International Conference on Dependable Systems and Their Applications (DSA)*, 2021, pp. 213–219.

[13] T. D. Gillespie, *Fundamentals of vehicle dynamics (Vol. 114)*. SAE Technical Paper, 1992.

[14] T. Takahama and D. Akasaka, "Model predictive control approach to design practical adaptive cruise control for traffic jam," *International Journal of Automotive Engineering*, vol. 9, no. 3, pp. 99–104, 2018.

APPENDIX

As mentioned in planar motion, the coordinates to describe the vehicle motion are X, Y, and Ψ, where (X, Y) represent the inertial coordinates of the location of the center of gravity of the vehicle, while Ψ (yaw angle) indicates the orientation of the vehicle-fixed frame about the Earth-fixed z-axis. The vector V is the velocity at the CG of the vehicle and makes a slip angle (β) with the longitudinal axis of the car. With the car in an absolute inertial frame, the motion equations are:

$$\dot{\chi} = Vcos(\Psi + \beta) \tag{43}$$

$$\dot{\Upsilon} = Vsin(\Psi + \beta) \tag{44}$$

$$\dot{\Psi} = \frac{Vcos(\beta)}{lf + lr} \tan(\delta) \tag{45}$$

Where χ and Υ are the longitudinal and lateral velocities, Ψ (yaw rate) is the vehicle angular velocity about the vehicle z-axis, δ is the steering angle, lf, and lr are the longitudinal distance from the CG to front and rear wheel, respectively.

For all the following equations in this section, we need both specific formulas to be applied to front-wheel f and another for rear-wheel r because both have different behaviors and functions of displacement in space.

All object displacement in space, in a frame of time, it is possible to extract all adding moments (Mx, My, Mz) and forces (F_x, F_y, F_z). These moments and forces pulled around the vertical axis at the CG represent all the vehicle's lateral motion and rotational dynamics according to three coordinates and DOF. In other words, to extract the acceleration (lateral and longitudinal), we need to use Newton's equations for translational motion in χ and Υ. This will allow us to obtain the vehicle's longitudinal and lateral motion equations. On the other hand, the z-axis uses Euler's equations to describe the angular motion. All these equations aim to describe the object's displacement in the lateral motion.

$$m\ddot{\chi} = m\dot{\Upsilon}\dot{\Psi} + F_{xf} + F_{xr} + F_{x\ ext} \tag{46}$$

$$m\ddot{\Upsilon} = m\dot{\Upsilon}\dot{\chi} + F_{yf} + F_{yr} + F_{y\ ext} \tag{47}$$

$$I_{zz}\ddot{\Psi} = l_f F_{yf} - l_r F_{yr} + M_{z\ ext} \tag{48}$$

Where $\ddot{\chi}$ and $\ddot{\Upsilon}$ represent longitudinal and lateral accelerations, $\ddot{\Psi}$ is angular acceleration and m is the vehicle's mass. F_{xf} and F_{xr} are the longitudinal forces applied to the front and rear wheels respectively. In contrast, F_{yf} and F_{yr} are the lateral forces of the front and rear wheels. $F_{x\ ext}$ and $F_{y\ ext}$ are the external forces applied to vehicle CG. I_{zz} is the yaw polar inertia. Finally, $M_{z\ ext}$ is the external moment of the vehicle CG about the vehicle z-axis.

Longitudinal and lateral forces applied to the front and rear wheels are calculated using longitudinal and lateral tire forces and the steering angle. We can see that the force of the rear wheels is logically simply the traction force of tires for longitudinal displacement F_l, while the lateral displacement of the rear wheel is equal to the cornering force of tires F_c. This is because only the front wheel can rotate when steering. On the other hand, the front wheel forces will be determined by the difference between the angles of traction force and cornering force.

$$F_{xf} = F_{lf}\cos(\delta) - F_{cf}\sin(\delta) \tag{49}$$

$$F_{yf} = F_{lf}\sin(\delta) - F_{cf}\cos(\delta) \tag{50}$$

$$F_{xr} = F_{lr} \tag{51}$$

$$F_{yr} = F_{cr} \tag{52}$$

Furthermore, traction directly results from the longitudinal force generated by tiers during acceleration (negative or positive). In contrast, the tire slip angles α and linear cornering stiffness C_y influence the tire's lateral force generated while cornering. It is also necessary to take into account the wheel friction coefficient μ and the normal force applied to the vehicle in the z-axis F_z over the nominal normal force applied to axles along the vehicle z-axis F_{znom}. These last two represent the forces that impact the tire that originate from the yam rotation.

$$F_{lf} = F_{xf\ input} \tag{53}$$

$$F_{lr} = F_{xr\ input} \tag{54}$$

$$F_cf = -C_{yf}\alpha_f\mu_f\frac{F_{zf}}{F_{znom}} \tag{55}$$

$$F_{cr} = -C_{yr}\alpha_r\mu_r\frac{F_{zr}}{F_{znom}} \tag{56}$$

To maintain pitch and roll equilibrium, the normal forces obtained by the following equations are divided by the nominal normal load to vary the effective friction parameters during vehicle weight and load transfer. All forces or moments that act over the vehicle CG about the vehicle axis need to be considered, including external forces.

$$(l_f+l_r)F_{zf} = l_r mg - (\ddot{\chi} - \dot{\Upsilon}\dot{\Psi})mh + hF_{xext} + l_r F_{z\ ext} - M_{y\ ext} \tag{57}$$

$$(l_f+l_r)F_{zr} = l_f mg - (\ddot{\chi} - \dot{\Upsilon}\dot{\Psi})mh + hF_{xext} + l_r F_{z\ ext} - M_{y\ ext} \tag{58}$$

Where h is the height of vehicle CG above the axle plane, $F_z\ ext$ is the external force applied to vehicle CG along the vehicle z-axis, $M_{y\ ext}$ is the external moment of the vehicle CG about the vehicle y-axis.

Finally, the slip angle of the tires (front and rear) represents the angle between the wheel velocity and the direction of the wheel itself.

$$\alpha_f = \arctan\frac{\Upsilon + l_f\Psi}{\chi} - \delta \tag{59}$$

$$\alpha_r = \arctan\frac{\Upsilon - l_r\Psi}{\chi} \tag{60}$$